Barrier to Rotation around the C_{sp^2}-C_{sp^2} Bond of the Ketoaldehyde Enol Ether MeC(O)CH═CH−OEt As Determined by ^{13}C NMR and ab Initio Calculations

Hans-Christian Siebert,*,† Emad Tajkhorshid,*,‡ and Janusz Dabrowski§

Bijvoet Center for Biomolecular Research, Department of Bio-Organic Chemistry, Utrecht University, P.O. Box 80.075, NL-3508 TB Utrecht, The Netherlands, Department of Molecular Biophysics, German Cancer Research Center, Im Neuenheimer Feld 280, D-69120 Heidelberg, Germany, and Max Planck Institute for Medical Research, Jahnstrasse 29, D-69120 Heidelberg, Germany

Received: December 13, 2000; In Final Form: July 2, 2001

NMR measurements and ab initio calculations were applied to determine the barriers to rotation around formally single bonds of the title methyl-β-ethoxyvinyl ketone, i.e., the vinylogue of the ethyl ester of acetic acid. For comparison, ab initio calculations were performed for α,β-unsaturated, β-N, and β-S substituted ketones. The relative height of the rotational barriers for $C_{sp^2}-C_{sp^2}$ and $C_{sp^2}-X$ bonds of the MeC(O)−CH═CH−X−alkyl(s) analogues was found to be reverse for X = N(alkyl)$_2$ vs X = O-alkyl or X = S-alkyl. This finding is discussed in terms of differences in the electron density distribution in these molecules, resulting from differences in electron-donating properties of the heteroatoms N, O, and S.

Introduction

α,β-Unsaturated ketones are polar molecules with partially equalized single and double bonds. The degree of the equalization strongly depends on the substituent at the β carbon atom. For example, the double bond measure for the formally single $C_{sp^2}-N$ and $C_{sp^2}-C_{sp^2}$ bonds of β-dialkylamino vinyl ketones and aldehydes, i.e., the vinylogues of amides, are high enough to enable one to observe hindered rotation around the former bond in ^1H NMR spectra recorded slightly below the ambient temperature, and that around the latter bond at moderately low temperatures.[1] In contrast, no hindered rotation was observed under comparable conditions for β-alkoxy substituted derivatives, i.e., the vinylogues of carboxylic esters, although their four rotamers were unambiguously determined at room temperatures with the aid of infrared spectroscopy[2] thanks to its favorable time scale (Scheme 1).

In this study we take advantage of the favorable ^{13}C NMR time scale[3,4] for determining the rotation barriers of the title alkoxy compound. It turned out that even at the lowest experimentally attainable temperature of 138 K only one of the rotations was frozen, namely that for the $C_{sp^2}-C_{sp^2}$ single bond. Thus, the barrier to rotation around this bond was higher than that for the $C_{sp^2}-O$ bond. This means that the sequential order of the two activation energies for the alkoxy compound is reverse as compared with that for dialkylamino analogues. This difference has been reproduced by ab initio calculations, and accounted for by different electron density distribution in the two types of molecules, i.e., by different electron-donating properties of oxygen and nitrogen to contribute to the polar resonance structures. In the case of the alkthio compound the ab initio calculations led to the smallest barriers to rotation. Comparable to the situation with alkoxy derivatives, the rotational barrier for the $C_{sp^2}-S$ bond is smaller than that for the $C_{sp^2}-C_{sp^2}$ bond.

Several model molecules of vinylogues of esters of carboxylic acids, amides, and alkthioesters were used for the computational part of the study (Scheme 2).

These compounds differ only in the heteroatom and its alkyl substituents. To simplify the description of the molecules in question, we will refer to them by a name specifying only the heteroatom and the alkyl groups. The O-ethyl compound **1**, which has been investigated experimentally in this paper, is the main molecule in our study. However, to compare the possible effect of the different properties of the heteroatoms on the rotation around different bonds, N-diethyl **2** and S-ethyl **3** compounds were also included in the calculations.

To examine and validate the reliability of the applied method, several different computational techniques were then used, and the results compared. Because of the expense of these calculations, the ethyl substituent was replaced by the methyl one. As will be described in detail below, this replacement did not influence the calculated barriers, but provided a simpler, less costly model for high level ab initio geometry minimizations, calculation of second derivatives, and transition state (TS) optimization. These calculations were performed only for O-methyl **4** and N-dimethyl **5** compounds.

The rotation barriers for the parent compounds of the vinylogues **1**−**5**, i.e., for esters, carboxylic acids, amides, and thioesters, have been investigated by several research groups using a number of experimental and computational methods.[5−12]

Methods

NMR Measurements. The synthesis of the title methyl-β-ethoxyvinyl ketone (**1**) is described elsewhere.[2] Its ^{13}C-spectra were recorded at 303 K (Figure 1) and at thirteen temperatures in an interval between 138 and 223 K, and two ^1H-spectra were

* Corresponding authors. For NMR information, correspondence should be addressed to Hans-Christian Siebert at Bijvoet Center for Biomolecular Research, Department of Bio-Organic Chemistry, Utrecht University, P.O. Box 80.075, NL-3508 TB Utrecht, The Netherlands; E-mail: hcsiebert@aol.com. For calculations, correspondence should be addressed to Emad Tajkhorshid at the author's current address at Theoretical Biophysics Group, Beckman Institute, University of Illinois at Urbana-Champaign, 405 N. Mathews, Urbana, IL 61801; E-mail: emad@ks.uiuc.edu.

† Utrecht University.

‡ German Cancer Research Center.

§ Max Planck Institute for Medical Research.

10.1021/jp004476g CCC: $20.00
Published on Web 08/22/2001

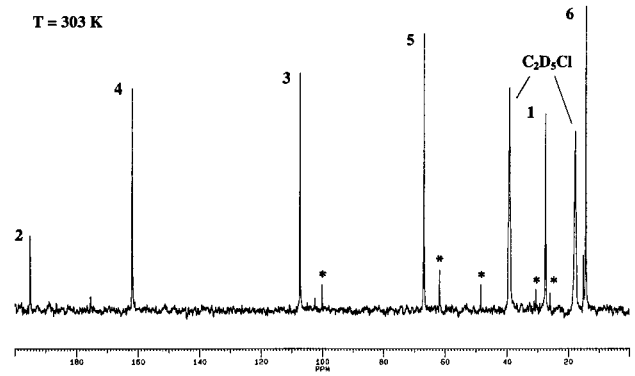

Figure 1. One-dimensional ^{13}C-spectrum of methyl-β-ethoxyvinyl ketone (**1**) at 303 K. Impurities are indicated (*).

SCHEME 1: The Rotamers of the Trans (E) β-alkoxy Vinyl Ketones;[2] for the Title Compound (1), $R^a = CH_3$, $R^b = C_2H_5$. The *s*-cis/*s*-trans notation refers to the cis/trans position of the C=C and C=O double bonds relative to the single bond between them. Correspondingly, O-*s*-cis/O-*s*-trans refers to the cis/trans position of the C=C and O−CH_2 bonds relative to the single bond between them.

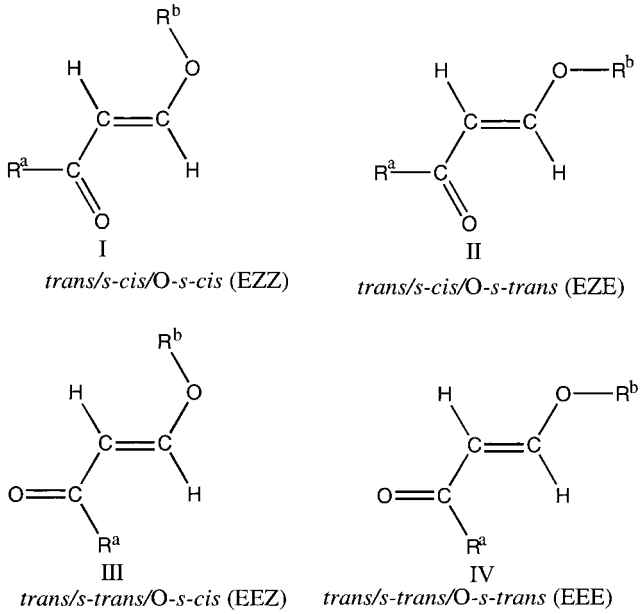

SCHEME 2

$$H_3C^1\text{-}C^2(=O)\text{-}C^3H=C^4H\text{-}X$$

1 X = OC_2H_5 **4** X = OCH_3

2 X = $N(C_2H_5)_2$ **5** X = $N(CH_3)_2$

3 X = SC_2H_5

recorded at 158 and 283 K. All experiments were carried out on a Bruker AM-500 NMR spectrometer, operating at 125 and 500 MHz, respectively. For ^{13}C-experiments, **1** was dissolved in deuterated ethyl chloride-d_5, whose melting and boiling points are at 137 and 285 K, respectively. The validity of temperature readings between 313 and 175 K was controlled by methanol calibration. The readings below 175 K can safely be assumed correct, since a sample of pure ethyl chloride crystallized exactly

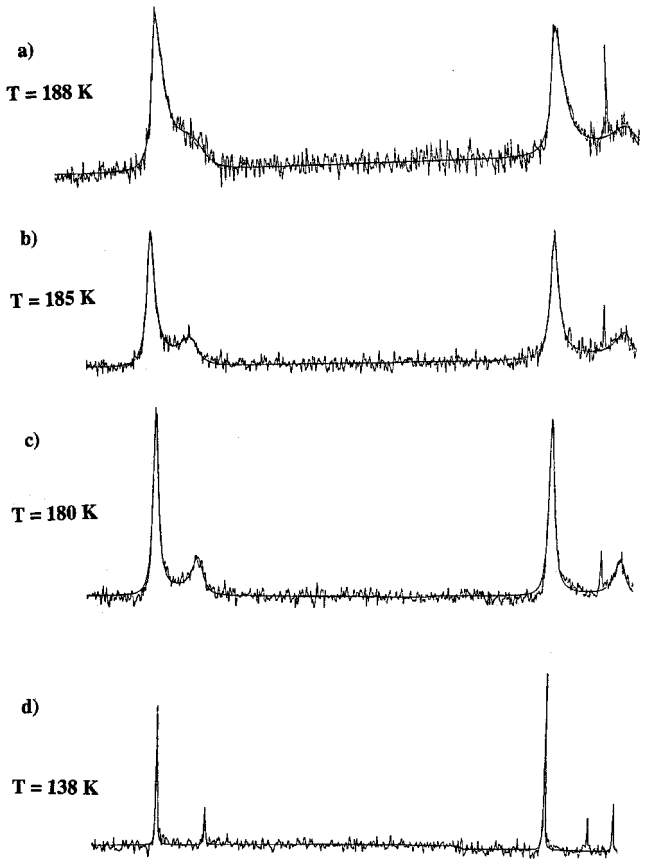

Figure 2. Line-fit of the C^3 and C^4 carbon signals derived by use of the DNMR-5 program. The signal which is caused by an impurity is is sharp in all of the four spectra.

at its melting point of 137 K, as observed by instantaneous disappearance of the FID and the lock signal.

T_1 inversion−recovery and T_2 spin−echo experiments,[13] performed at several temperatures, showed that all measured signals were determined for a fully relaxed state. Comparing the T_2 values thus obtained with values derived from line-widths we found that the line-shape analysis was not affected by the strong temperature dependence of the T_2 parameter.

Inverse gated decoupling experiments[14] were carried out in order to ascertain that the *s*-cis and *s*-trans populations determined by integration of their signals were not influenced by NOE.

The line shape analysis, shown in Figure 2 for four representative temperatures, was performed with the DNMR-5 program[3,4] on a CDC-Cyber 175-Computer. Theoretical spectra were fitted to the corresponding spectra measured at thirteen temperatures in the 138−223 K interval, thus yielding the respective rate constants k [s^{-1}] of the isomerization observed. The resulting data which were obtained by this analysis are displayed in Tables 1 and 2.

Computational Methods

All ab initio calculations were performed with application of the GAUSSIAN 94 program.[15] To scan the potential energy surface (PES) representing the rotation around different bonds, the torsion angles were changed in 15.0° increments from 0.0° (*s*-cis or X-*s*-cis) to 180.0° (*s*-trans or X-*s*-trans) conformation. The barrier against a given rotation was then calculated as the difference between the highest point on the PES (90°-rotated species in majority of the cases) and the corresponding more stable planar form. The majority of the barriers were calculated

TABLE 1: Populations of the *s*-Cis (P1) and *s*-Trans (P2) Conformers, Free Energy Differences, *s*-Cis to *s*-Trans Rates and Their Standard Deviations for the Title Compound 1, As Obtained from the NMR Analysis

T [K][a]	$P1$:$P2$[b]	ΔG^{0c}	k [s^{-1}][d]	Δk
223	0.64:0.36	0.25	22600	1120
213	0.66:0.34	0.27	9790	199
203	0.67:0.33	0.28	2611	62.0
193	0.68:0.32	0.28	668	20.4
188	0.69:0.31	0.30	371	9.8
186	0.69:0.31	0.30	313	13.0
185	0.69:0.31	0.30	239	7.7
183	0.70:0.30	0.30	212	5.0
180	0.70:0.30	0.30	142	2.9
175	0.71:0.29	0.30	81.4	1.6
165	0.73:0.27	0.32	49.8	1.2
143	0.77:0.23	0.34	5.6	1.3
138	0.78:0.22	0.34	0.0	

[a] All temperatures in Kelvin. [b] Obtained by signal integration; for temperatures close to and above coalescence, the populations were extrapolated according to the Boltzmann distribution. [c] All free energy values are given in kcal/mol. [d] The *s*-cis to *s*-trans rates were calculated by line-shape analysis.

TABLE 2: The Gibbs Free Energy Differences (kcal/mol) between the *s*-Cis or *s*-Trans Conformer and the Corresponding Activated State at Different Temperatures, As Obtained by the Eyring Plot. For Comparison, the Temperature-Dependent $\Delta H^{\#}$ *s*-Cis and $\Delta H^{\#}$ *s*-Trans Values Were Derived by the Analysis of the Arrhenius Plot

T [K][a]	$\Delta G^{\#}$*s*-cis[b]	$\Delta G^{\#}$*s*-trans[b]	$\Delta H^{\#}$*s*-cis[b]	$\Delta H^{\#}$*s*-trans[b]
223	8.62	8.37	7.95	7.47
213	8.59	8.32	7.97	7.49
203	8.56	8.28	7.99	7.51
193	8.52	8.24	8.01	7.53
188	8.51	8.21	8.02	7.54
186	8.50	8.20	8.03	7.55
185	8.50	8.20	8.03	7.55
183	8.49	8.19	8.03	7.55
180	8.48	8.18	8.04	7.56
175	8.46	8.16	8.05	7.57
165	8.43	8.11	8.07	7.59
143	8.36	8.02	8.11	7.63
138	8.34	8.00	8.12	7.64

[a] All temperatures in Kelvin. [b] All free energy values are given in kcal/mol.

using density functional theory (DFT). All of the DFT calculations were performed using the Becke3LYP (B3LYP) hybrid functional and 6-31G(d,p) basis set including polarized functions on both the hydrogen and heavy atoms. To assess the validity of the calculations, a number of rotations was also studied at the MP2/6-31G(d,p) level of theory. Furthermore, to examine the effect of the dielectric response of the medium on the calculated barriers, the calculations were repeated for one compound using the Onsager model, which implicitly includes the electrostatic response of a solvent into the calculation through screening of the electrostatic interactions. For these calculations, a dielectric constant of 78.4, corresponding to that of an aqueous solution, was used.

Several points on the PES were located by fixing the dihedral angle of interest at different values. The calculations were performed with three different sets of constraints. In all of these sets, the dihedral angle d formed by four heavy atoms ($C^1-C^2_{carbonyl}-C^3=C^4$ for the rotation around the $C_{sp^2}-C_{sp^2}$ bond, and $C^3=C^4-X-C_{alkyl}$ for the rotation around the C^4-X bond) were changed in 15 degree increments, and at each dihedral angle the geometry was optimized. In the first set of constraints (set **a**), which has been also used for the calculation of the barriers in ethylated species **1**, **2**, and **3** (Table 3), the hydrogen atoms neighboring the rotation axis (the H atom on C^3 for the rotation around the $C_{sp^2}-C_{sp^2}$ bond, and the H atom on C^4-H for the rotation around the C^4-X bond) are also kept in the plane formed by the adjacent heavy atom (C^3 or C^4) and the rotation axis. In set **b**, all hydrogen and heavy atoms linked to the rotation axis are forced to be in-plane, and in set **c**, only dihedral angle d is fixed, and all other degrees of freedom can relax.

TABLE 3: Relative Energies (kcal/mol) for Different Points on the PES of the Rotation around the $C_{sp^2}-C_{sp^2}$ and C−X Single Bonds in Ethylated Compounds, Calculated Using B3LYP/6-31G(d,p) Method. The Energies Are Relative to the Energetically Most Favorable Conformer

dihedral angle d[a]	O-ethyl		N-diethyl		S-ethyl	
	$C_{sp^2}-C_{sp^2}$	C−O	$C_{sp^2}-C_{sp^2}$	C−N	$C_{sp^2}-C_{sp^2}$	C−S
0.0	0.0	0.0	0.0	0.0	0.0	0.0
15.0	0.6	0.7	0.8	0.8	0.6	0.6
30.0	2.4	2.6	3.0	3.0	2.3	2.2
45.0	5.0	5.1	6.4	6.2	4.8	4.2
60.0	7.9	7.2	10.1	9.8	7.3	5.9
75.0	10.2	8.3	13.2	13.3	9.2	6.8
90.0	11.2	8.2	14.5	16.0	10.0	6.6
105.0	10.7	7.0	13.8	17.6	9.6	5.6
120.0	8.9	5.3	11.4	7.0	8.1	4.2
135.0	6.6	3.5	8.4	4.0	6.0	2.6
150.0	4.4	2.1	5.5	1.8	4.0	1.5
165.0	2.8	1.3	3.3	0.4	2.3	0.9
180.0	2.1	1.1	2.5	0.0	1.7	0.7

[a] Constraint set **a** is used: at each point dihedral angle d is fixed, and the hydrogen atoms neighboring to the central bond are kept in plane.

The default optimization criteria of the GAUSSIAN 94 program[15] were used for all of the geometry optimizations.

Results and Discussion

Dynamic NMR Experiments. To ascertain whether the rotation around $C^4_{sp^2}-O$ or rather the $C^2_{sp^2}-C^3_{sp^2}$ bond is frozen at low temperatures, ^{1}H-NMR spectra of **1** ($H_3C^1-C^2(=O)-C^3H=C^4H-O-C^5H_2-C^6H_3$) were measured and compared with those of methyl-β-dimethylaminovinyl ketone (**5**) [$(H_3C^1-C^2(=O)-C^3H=C^4H-N(C^{5,5'}H_3)_2$].[1] There are sharp signals for all protons in the spectrum of **5** recorded at 302 K, which reflexes fast rotation in all parts of the molecule. At 260 K the signal of the two methyl groups linked to N is split in two, due to lowering of the rate of rotation around the C−N bond. At 215 K these signals, as well as those of the C^3H and C^4H protons, are additionally split because of the frozen rotation around the $C^2_{sp^2}-C^3_{sp^2}$ bond. In contrast, the low temperature (158 K) spectrum of **1** shows the C^5-H signal but slightly broadened, whereas the formerly sharp $C^3_{sp^2}-H$ and $C^4_{sp^2}-H$ signals are split into two components each. A similar picture is observed in low-temperature ^{13}C spectra of **1**. It can therefore be concluded that only the rotation around the $C^2_{sp^2}-C^3_{sp^2}$ bond is frozen, and the two components of each split signal correspond to the *s*-cis and *s*-trans rotamers of **1**. This conclusion is convincingly supported by the ab initio calculated barrier for this rotation which is higher by 2.9 kcal/mol than the alternative barrier for the $C^4_{sp^2}-O$ bond (Table 3).

It was shown in previous work[2] on α,β-unsaturated systems that steric strain due to the interaction between the alkyl substituent (here H_3C^1; see also Scheme 1) and the C^4-H olefinic proton in the *s*-trans rotamer induces a shift of the equilibrium toward the *s*-cis form, where this alkyl opposes the C^3-H olefinic proton at a larger distance. Such is the case with **1**; for

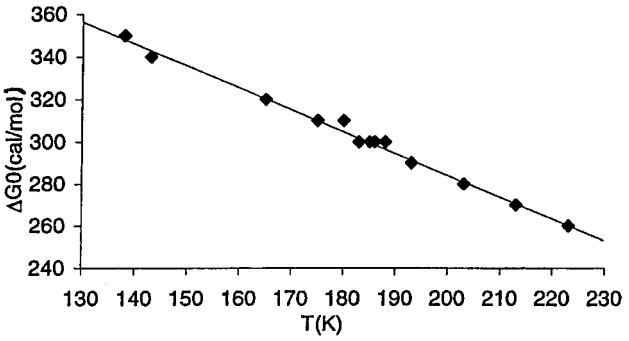

Figure 3. The determination of the ΔH^0 and the $\Delta S°$ value by linear regression with the formula $\Delta G^0 = \Delta H^0 - T\Delta S°$. The temperature-dependent ΔG^0 values are given in Table 1.

the ab initio optimized geometries of its four rotamers the distances in question are as follows:

C^1-H/C^3-H:	C^1-H/C^4-H:
s-cis/O-*s*-cis: 2.73 Å	*s*-trans/O-*s*-cis: 2.54 Å
s-cis/O-*s*-trans: 2.73 Å	*s*-trans/O-*s*-trans: 2.60 Å

The markedly larger distance of 2.73 Å points to the *s*-cis conformation as the predominant one of lower energy. The corresponding energy values are given in Table 3 and discussed in the next section. The temperature-dependent populations of the *s*-cis and *s*-trans rotamers were determined by integration of the corresponding ^{13}C signals. For temperatures close to and above coalescence the ratio of these populations were extrapolated according to the Boltzmann distribution. The values thus obtained were practically the same as those calculated by iteration with use of the DNMR-5 program[3,4] (Table 1).

The $\Delta G° = RT \ln [P1]/[P2]$ values, also monitored in Table 1, were calculated, and the $\Delta H° = 0.48$ kcal/mol and $\Delta S^0 = 1.00$ cal/(mol K) values for the nonactivated state were obtained by linear regression according to $\Delta G^0 = \Delta H^0 - T\Delta S°$ (Figure 3). The temperature-dependence of the *s*-cis/*s*-trans population ratios are displayed in Table 1. The DNMR-5 program[3,4] also delivers the temperature-dependent *k*-rates and the corresponding standard deviations Δk by fitting the calculated spectrum to the experimental one. The corresponding values are shown in Table 1. The line-fit for the C^3 and C^4 carbon signals recorded at four representative temperatures is shown in Figure 2.

The activation energy of $E_a = 8.39$ kcal/mol and the k_0-rate of 2.79×10^{12} were determined by linear regression as a result of the Arrhenius plot analysis, which relies on eleven $k[T]$ values in an interval of 58 K between 223 and 165 K. Application of the formula $\Delta H^{\#} = E_a - RT$ led to temperature-dependent enthalpic values $\Delta H^{\#}$ of the transition state (Table 2). The Eyring plot analysis (Figure 4) was carried out in order to obtain the temperature-dependent $\Delta G^{\#}$ values as well as the temperature-independent $\Delta H^{\#}$ and $\Delta S^{\#}$ values for the *s*-cis conformer. Of the thirteen experimental $k[T]$ values measured in an interval of 80 K between 223 and 143 K (Figure 2), that for 138 K was excluded because of its high deviation (Figure 4). Following results were derived by this analysis: $\Delta H^{\#}_{s-cis} = 7.88$ kcal/mol (SD = 0.56 kcal/mol) and $\Delta S^{\#}_{s-cis} = -3.33$ cal/(mol K) {SD = −2.91 cal/(mol K)).

The thermodynamic parameters $\Delta H^{\#}_{s-trans}$ and $\Delta S^{\#}_{s-trans}$ for the *s*-trans conformer were calculated by subtracting the $\Delta H° = 0.48$ kcal/mol and the $\Delta S^0 = 1.00$ cal/(mol K) value of the nonactivated state from the enthalpy and entropy value of the *s*-cis conformer. Thereby one obtains: $\Delta H^{\#}_{s-trans} = 7.40$ kcal/mol and $\Delta S^{\#}_{s-trans} = -4.33$ cal/(mol K). The temperature-dependent $\Delta G^{\#}$ values of the *s*-cis and *s*-trans state (calculated with $\Delta G^{\#} = \Delta H^{\#} - T\Delta S^{\#}$) are listed in Table 2.

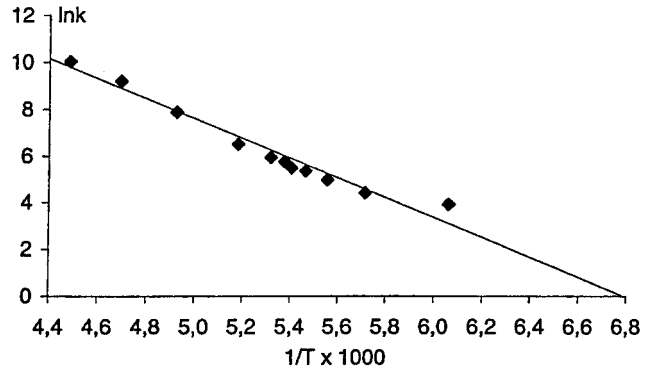

Figure 4. Eyring plot analysis for the determination of $\Delta G^{\#}$, $\Delta H^{\#}$, and $\Delta S^{\#}$ values for the *s*-cis state. The analysis bases on twelve $k[T]$ values in an interval of 80 K between 223 and 143 K. The temperature-dependent $\Delta G^{\#}$ values for the *s*-cis and *s*-trans state are listed in Table 2.

The experimentally obtained negative entropy value $\Delta S^{\#}$ for **1** may suggest specific interactions between solute and solvent molecules resulting in a more ordered transition state than in the planar forms. These interactions can be of steric and electrostatic nature.[12]

Quantum Chemical Calculations

The rotations under study were those around the C^2-C^3 ($C_{sp^2}-C_{sp^2}$) and C^4-X single bonds, which have a significant partial double bond character due to the conjugation between the π-electrons of the alternate double bonds and the lone electron pair(s) of the heteroatom. The bond order and the rotational barrier vary with different X substituents, depending on the extent of electron delocalization. The applicability of the B3LYP method to the study of the rotation around single bonds and to the description of the 90°-rotated transition state species has been previously shown in studies of polyene systems.[16−19]

As will be seen later, the barriers calculated with use of the B3LYP hybrid functional are in all cases larger than those obtained from the experiments. This difference may be due to overestimation of the conjugation in DFT (when compared to multi-configurational SCF calculations) that we have observed and briefly discussed elsewhere.[18,20] A final word with regard to this problem requires, however, a systematic comparison of different computational methods. In the present study we have verified the DFT results by comparison of a few cases with MP2 calculations. We have examined both the rotations around the $C_{sp^2}-C_{sp^2}$ and C^4-X single bonds in smaller models (**4** and **5**) at the MP2/6-31G(d,p) level of theory. This resulted in barriers that are slightly closer in magnitude to the experimental values. The differences between the theoretical and experimental barriers amount to 1−2 kcal/mol. Comparable differences between the experimental and theoretical values of the rotational barriers (about 1 kcal/mol) have been reported in the already cited paper,[12] and discussed in terms of solvent field vs direct solvation effect.

Rotational Barriers in X−Ethyl Species. The electronic energy for different points on the PES for the rotations around the $C_{sp^2}-C_{sp^2}$ and C−X bonds in molecules **1**, **2**, and **3** are compiled in Table 3 and graphically shown in Figures 5 and 6, respectively. For all three molecules, the *s*-cis conformer is the energetically favorable one, hence the *s*-cis to *s*-trans isomer-

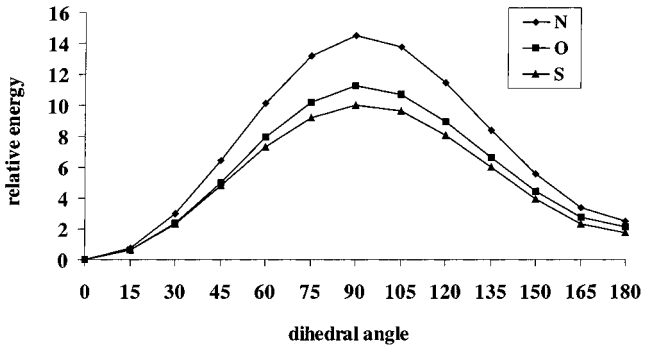

Figure 5. Potential energy curve of the rotation around the $C_{sp^2}-C_{sp^2}$ single bond in ethylated compounds **1**−**3**. Relative energies (kcal/mol) for different points were calculated using the B3LYP/6-31G(d,p) method. The energies are relative to the energetically favorable *s*-cis conformer.

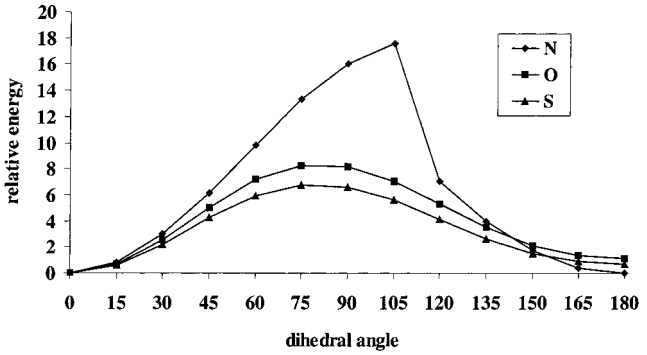

Figure 6. Potential energy curve of the rotation of C−X (X = N, O, S) single bonds in ethylated compounds **1**−**3**. Relative energies (kcal/mol) for different points were calculated using the B3LYP/6-31G(d,p) method. The energies are relative to the energetically favorable *s*-cis conformer.

ization barriers are higher than those for the reverse process, as demonstrated here for the title compound **1** by NMR experiments. These higher barriers were calculated for compounds **1**−**3**. For both rotations, the highest barriers are observed for the amide vinylogue **2** (14.5 and 17.6 kcal/mol for the $C_{sp^2}-C_{sp^2}$ and C−X bonds, respectively). This can be accounted for by the higher polarizability of the lone electron pair of nitrogen, as compared with those of oxygen and sulfur. Most important, the numbers for the ester vinylogue **1** (11.2 kcal/mol for the $C_{sp^2}-C_{sp^2}$ bond and 8.3 kcal/mol for the C−O bond) reproduce the experimentally ascertained reverse sequential order of these activation energies vs those for **2**. The barriers calculated for compound **3** (10.0 and 6.8 kcal/mol for the $C_{sp^2}-C_{sp^2}$ and C−S bonds, respectively), are the lowest ones because of the lower capability of sulfur to donate its lone electron pairs to π-electronic systems.[21] This trend has also been shown in studies comparing the effect of oxygen and sulfur on the barriers against the rotation around delocalized double bonds.[22]

In agreement with the relative heights of the barriers for compounds **1** and **2**, calculation of fully optimized geometries showed a shortened $C_{sp^2}-C_{sp^2}$ single bond, and elongated C═O and C^3═C^4 double bonds for **2** (1.464, 1.363, and 1.231 Å, respectively) relative to **1** (1.474, 1.346, and 1.227 Å, respectively), indicating a larger extent of delocalization for **2**. Because of reverse transfer of σ electrons, the change of atomic charges along the unsaturated chain may not properly reflect the level of π-electron delocalization. Nevertheless, examination of the atomic charges for the ground and transition state presented in Table 4 allows one to draw some tentative conclusions regarding the electronic effects involved in the rotational barriers. For both

TABLE 4: Comparison of Charge Distribution in Compounds 1 and 2 at Different conformations. Each charge (*e*) Is the Sum of the Charges on the Heavy Atom(s) and All Hydrogen Atoms Connected to It (them)

compound **1**				compound **2**			
atom/group	planar	TS1	TS2	atom/group	planar	TS1	TS2
methyl	−0.01	+0.01	−0.00	methyl	−0.03	−0.00	−0.01
C(carbonyl)	+0.41	+0.37	+0.41	C(carbonyl)	+0.41	+0.36	+0.41
O(carbonyl)	−0.49	−0.41	−0.47	O(carbonyl)	−0.51	−0.42	−0.47
C_α	−0.12	−0.08	−0.06	C_α	−0.15	−0.12	−0.04
C_β	+0.36	+0.31	+0.31	C_β	+0.29	+0.24	+0.22
O_γ	−0.46	−0.47	−0.49	N_γ	−0.40	−0.41	−0.45
ethyl	+0.31	+0.29	+0.29	ethyl 1	+0.20	+0.18	+0.17
				ethyl 2	+0.20	+0.17	+0.16

the molecules **1** and **2**, the rotation around the $C_{sp^2}-C_{sp^2}$ bond (TS1) leads to essentially complete breakdown of the conjugation between the carbonyl and substituted vinyl moieties. This π-electron separation causes that the two moieties acquire less differentiated polarization in the TS1 state; the positive charge of the carbonyl carbon atom decreases and the negative charge of the oxygen becomes less negative. The same is observed for carbon atoms of the vinyl group. Interestingly, since at the transition state TS2 the π-interaction with the X heteroatom is at a minimum, the identical remaining $H_3C-C(=O)-CH=CH-$ parts of the structures of **1** and **2** can be expected to show a very similar electron distribution. This is indeed the case; the +0.41 *e* charge of the remote C^2 (carbonyl) and the −0.47 *e* charge of the O (carbonyl) are identical for **1** and **2**, and the charges of the vinyl C_α differ only slightly (−0.04 *e* for **1** and −0.06 *e* for **2**). The large difference for the C_β atom directly bonded to the heteroatom X (+0.31 *e* for **1** and +0.22 *e* for **2**) will require a more rigorous treatment, as applied by Wiberg et al. in a series of papers on the interaction of carbonyl groups with substituents.[5,21,23]

Returning to the problem of the barriers' heights, the larger electron population of the more negative O_γ (−0.46 *e*) as compared with N_γ (−0.40 *e*) points to a much lower participation of the former in the conjugation with the remaining part of the molecule, and hence results in a lower C−O barrier.

Whereas the maximum point on the PES of the rotation around $C_{sp^2}-C_{sp^2}$ bonds is found at the 90°-rotated species (Figure 5), the corresponding point during the rotation around C−X bonds are located at slightly different dihedral angles (Figure 6). In compounds **1** and **3**, the maximum is observed at 75°-rotated species, however, the energy is practically equal to that of the corresponding 90°-rotated species of these molecules. In the case of the rotation around the C−N bond in **2**, the energy maximum is found at the dihedral angle of 105°, being about 1.5 kcal/mol higher in energy than the 90°-rotated species. This observation is related to the pyramidalization of the nitrogen atom during the rotation around the C^4-N bond. This rotation was induced by changing the dihedral angle *d* between the $N-C_{alkyl}$ bond (link between the nitrogen atom and one of the alkyl substituent on it) and the C^3═C^4 double bond. Except for this dihedral angle being fixed, all other degrees of freedom, including the conformation of the second ethyl group were free to relax during the geometry optimizations. In the starting (d = 0°) and final (d = 180°) geometries, the nitrogen atom has an sp^2-like hybridization (because of the contribution of its lone electron pair to the π-electronic system), and therefore forms a planar center. During the rotation around the C^4-N bond, however, the conjugation of the lone pair and the π-electrons decreases, and consequently the nitrogen atom recovers its sp^3 hybridization and converts to a pyramidal center. This is observed during the early steps of the rotation (at d = 15° or

TABLE 5: Comparison of the Relative Energies and Rotational Barriers (kcal/mol) Calculated by Different Methodologies for the Rotation around the $C_{sp^2}-C_{sp^2}$ and the C−O Single Bonds in O-Methylated Compound 4

method	rotation	E_{s-cis}	$E_{s-trans}$	$\Delta E^{\#}_{ct}$[a]	$\Delta E^{\#}_{tc}$[a]
B3LYP/6-31G(d,p)[b]	$C_{sp^2}-C_{sp^2}$	0.0	2.2	11.1	8.9
B3LYP/6-31G(d,p)[c]	$C_{sp^2}-C_{sp^2}$	0.0	2.2	11.2	9.0
B3LYP/6-31G(d,p)[d]	$C_{sp^2}-C_{sp^2}$	0.0	2.2	11.1	8.9
B3LYP/6-31G(d,p)[b] (zpe and thermal effects included)[e]	$C_{sp^2}-C_{sp^2}$	0.0	2.1	10.1	7.9
B3LYP/6-31G(d,p)[b] (TS optimization)[e]	$C_{sp^2}-C_{sp^2}$	0.0	2.2	11.1	8.9
B3LYP/6-31G(d,p)[b] (Onsager model)[f]	$C_{sp^2}-C_{sp^2}$	0.9	0.0	10.7	11.6
MP2/6-31G(d,p)[b]	$C_{sp^2}-C_{sp^2}$	0.0	2.0	9.6	7.6
B3LYP/6-31G(d,p)[b]	C−O	0.0	1.2	8.5[g]	7.3[g]
MP2/6-31G(d,p)[b]	C−O	0.0	2.0	8.2[h]	6.2[h]

[a] $\Delta E^{\#}_{ct}$ and $\Delta E^{\#}_{tc}$ are the barriers against *s*-cis to *s*-trans and *s*-trans to s-cis isomerizations, respectively. [b] Constraint set **a** is used: dihedral angle *d* is fixed, and the hydrogen atoms neighboring to the central bond are kept in plane. [c] Constraint set **b** is used: dihedral angle *d* is fixed, and all of the atoms neighboring to the central bond are kept in plane. [d] Constraint set **c** is used: only dihedral angle *d* is fixed, and all other degrees of freedom are fully relaxed. [e] The 90-degree rotated species included one imaginary frequency corresponding to the rotation around the $C_{sp^2}-C_{sp^2}$ single bond. Both *s*-cis and *s*-trans planar conformers were also characterized to be minimum after the examination of the second derivatives. [f] Onsager solvent model using the recommended radius and a dielectric constant of $\epsilon = 78.4$. [g] Observed at $d = 75$, 0.1 kcal/mol higher than at $d = 90$. [h] Observed at $d = 75$, 0.2 kcal/mol higher than $d = 90$.

30°). Further rotation approaching the TS region (observed at $d = 105°$) is accompanied with a nitrogen inversion resulting in a reverse pyramidal center located at the nitrogen atom. Due to this behavior, and because of plotting the energy values against the torsion angle of only one of the alkyl groups, the TS is found after passing the so-called "90°-rotated species". Starting from the final geometry ($d = 180°$) and rotating back the C^4-N bond to the conformer with $d = 0°$ results in the observation of the maximum energy at the point of $d = 75°$. Thus, there are two local minima on the multidimensional energy surface which correspond to the pyramidal NR_2 group. Essentially, the observed discontinuity is an artifact of the definition of the rotation angle; with the possibility of the pyramidalization of the NR_2 group its rotation should be studied on two-dimensional cross section of the complete energy surface of the molecule. This technical issue is a known difficulty in the study of such rotations in nitrogen-containing compounds, and have been discussed in previous studies.[24, 25]

Assessment of the Methods Used for the Calculation of Rotational Barriers. To validate the results obtained from the calculations described in the previous section, several technical issues have been examined by repeating the calculations using different methodologies. Because of the cost of the calculations, however, the ethyl substituents on the heteroatom were replaced by methyl ones. Only O-methyl **4** and N-dimethyl **5** molecules were used for further evaluation and assessment of the applied techniques.

The barriers against the rotation around the $C_{sp^2}-C_{sp^2}$ and C−X bonds in compounds **4** and **5**, calculated with different methods, are compiled in Tables 5 and 6**,** respectively. Comparison of these results with those compiled in Table 3 shows that the replacement of the ethyl group by a methyl one does not have any noteworthy influence on the rotational barriers. The maximum difference between the barriers calculated for methylated species (**4** and **5**), and the corresponding

TABLE 6: Comparison of the Relative Energies and Rotational Barriers (kcal/mol) Calculated by Different Methodologies for the Rotation around the $C_{sp^2}-C_{sp^2}$ and C−N Single Bonds in N-Dimethyl Compound 5

method	rotation	$E_{s-trans}$	E_{s-cis}	$\Delta E^{\#}_{ct}$[a]	$\Delta E^{\#}_{tc}$[a]
B3LYP/6-31G(d,p)[b]	$C_{sp^2}-C_{sp^2}$	2.1	0.0	13.6	11.5
B3LYP/6-31G(d,p)[c]	$C_{sp^2}-C_{sp^2}$	2.3	0.0	13.7	11.4
B3LYP/6-31G(d,p)[d]	$C_{sp^2}-C_{sp^2}$	2.3	0.0	13.7	11.4
B3LYP/6-31G(d,p)[b] (zpe and thermal effects included)[e]	$C_{sp^2}-C_{sp^2}$	2.4	0.0	12.6	10.2
MP2/6-31G(d,p)[b]	$C_{sp^2}-C_{sp^2}$	1.8	0.0	11.4	9.6
B3LYP/6-31G(d,p)[b]	C−N	0.1	0.0	17.0[f]	
B3LYP/6-31G(d,p)[c]	C−N	0.0	0.0	20.7[g]	
MP2/6-31G(d,p)[c]	C−N	0.0	0.0	19.7[g]	

[a] $\Delta E^{\#}_{ct}$ and $\Delta E^{\#}_{tc}$ are the barriers against *s*-cis to *s*-trans and *s*-trans to *s*-cis isomerizations, respectively. [b] Constraint set **a** is used: *d* is fixed, and the hydrogen atoms neighboring to the central bond are kept in plane. [c] Constraint set **b** is used: *d* is fixed, and all of the atoms neighboring to the central bond are kept in plane. Constraint set **c** is used: only dihedral angle *d* is fixed, and all other degrees of freedom are fully relaxed. [e] The 90-degree rotated species included one imaginary frequency corresponding to the rotation of the $C_{sp^2}-C_{sp^2}$ single bond. Both *s*-cis and *s*-trans planar conformers were also characterized to be minimum after the examination of the second derivatives. [f] Observed at 60-degree rotated species. [g] Because of the applied constraints, observed at 90-degree rotated species.

values for ethylated analogues (**1** and **2**) is observed for the rotation around the $C_{sp^2}-C_{sp^2}$ bond, and is less than 1.0 kcal/mol.

To examine if the calculated barriers could be influenced by the applied geometry constraints, the calculations were performed with three different sets of constraints, as described in the Methods section. The values presented in Tables 5 and 6 show that except for the rotation around the C^4-N bond in **5** no effect due to the application of different sets of the constraints was observed. In the case of the C−N rotation, application of set **b** prevents the nitrogen atom from pyramidalization, resulting in a 3.5 kcal/mol increase in the calculated barrier.

For both **4** and **5**, the effect of thermal energy corrections on the calculated barriers against the rotation around the $C_{sp^2}-C_{sp^2}$ bond was also examined. The energies used for the calculation of barriers were corrected by inclusion of zero-point and thermal energies. Because of the unimolecular nature of the reaction under study (isomerization), the values obtained after including the correction can be used as enthalpy differences. In both cases, a decrease of about 0.6−0.7 kcal/mol in the calculated barrier was obtained. The barrier against the rotation around the $C_{sp^2}-C_{sp^2}$ bond in **4** was also calculated after locating the TS by maximizing the energy with respect to the reaction coordinate (dihedral angle *d*). The TS was characterized by second derivative calculations and examination of the vibration corresponding to the negative eigenvalue. Comparison of the results shows that, at least for the rotation around $C_{sp^2}-C_{sp^2}$, the difference between the energy of the 90-degree rotated species and the planar forms provides a reasonable measure of the rotational barriers.

Comparison of the above results with the experimental values indicates a general overestimation of the calculated barrier heights. This is, however, mainly observed for the barrier against *s*-cis to *s*-trans isomerization. For instance, after inclusion of thermal energies, a barrier of 7.9 kcal/mol (Table 3) was calculated for the *s*-trans to *s*-cis isomerization around $C_{sp^2}-C_{sp^2}$ bond in compound **4**, in good agreement with the experimental $\Delta H^{\#}_{s-trans}$ value of about 7.5 kcal/mol (Table 2). A difference of about 2.0 kcal/mol was found, however, for

the barrier against *s*-cis to *s*-trans isomerization. The experimental $\Delta H^{\#}_{s-cis}$ value is about 8.0 kcal/mol (Table 2), whereas the calculated barrier amounts to 10.1 kcal/mol. This difference may be partly attributed to overestimation of the relative stability of the *s*-cis conformer in the calculations by about 2.0 kcal/mol. This is much larger than the observed experimental value of 0.48 kcal/mol derived from the population of the conformers.

Since this discrepancy might result from a tendency of DFT calculations to overestimate the delocalization effect in polarized, conjugated systems (vide supra), we repeated some of the calculations with the MP2/6-31G(d,p) level of theory. However, despite an improvement of the calculated barriers with respect to the experimental ones, the *energy differences* between the *s*-cis and *s*-trans conformers remained practically unchanged, amounting to 2.0 kcal/mol for **4** (Table 5) and 2.2 kcal/mol for **5** (Table 6).

We have also examined the magnitude of the solvent effects on the $C_{sp^2}-C_{sp^2}$ barrier in **4**. Rather than to focus on some particular solvent our calculations have been carried out with the dielectric constant $\epsilon = 78.4$ which can be expected to lead to the limiting values of the solvent effect. Despite the very large value of ϵ the nonspecific solvent solute interactions do not lead to significant effects on the rotational barrier. However, compared to the gas-phase ordering they reverse the order of stability for planar conformers (*s*-cis vs *s*-trans). After inclusion of the Onsager solvent model, the *s*-trans conformer becomes energetically more favorable by 0.9 kcal/mol (Table 5), whereas in all gas-phase calculations, the *s*-cis conformer is more stable by 1-2 kcal/mol. This effect is directly related to the dipole moment of the molecule in different conformations. In the *s*-cis form the dipole moment of **4** is 2.88 D, vs 5.44 D for the *s*-trans conformer. Therefore, the latter form has a much larger coupling to a polar environment and can be largely stabilized after the application of a solvent model. This should obviously result in different populations of these forms in different solvents.

The present results give the upper limit for changes due to solvent−solute nonspecific interaction and in general agree with earlier results obtained from the experimental measurements of the *s*-cis/*s*-trans ratio for enamino ketones in different solvents.[26] In this early report, the *s*-cis/*s*-trans ratio of 73/27 was found for the compound **5** in $CH_2{=}CCl_2$. In acetone, the ratio decreased to 50/50, and in methanol the *s*-trans conformer acquired a higher population of 64%. Hence, it can be expected that calculations with some intermediate value of ϵ could correctly reproduce the experimental small energy difference for the two conformers. However, the reason for the overestimation of the calculated absolute values of the rotational barriers can hardly be formulated at present, although can be hoped to be better understood with a further progress in calculations of solute−solvent interactions.

Conclusions

The title β-ethoxy vinyl ketone **1** is characterized by very low barriers to rotation around the $C_{sp^2}-C_{sp^2}$ and, particularly, $C_{sp^2}-O$ single bonds. This is contrary to the β-dialkylamino analogues with their high computational and the experimentally derived energy values, which show that the barriers to rotation are high, $C_{sp^2}-N$ barrier being higher than the $C_{sp^2}-C_{sp^2}$ one.

A noticeable entropy of the transition state of **1** and the solvent-dependence of both the calculated relative stabilities of the *s*-cis vs *s*-trans conformers and the isomerization barriers suggest that the dielectric factor and the specific interactions between the solute and the solvent molecules are likely to play an important role in the search for a satisfactory physical model of rotational barriers.

MP2 calculations resulted in rotational barriers that are closer to the experimentally determined ones.

Acknowledgment. We sincerely thank Prof. Dr. Andrzej J. Sadlej of the Nicolaus Copernicus University, Torun, Poland, for valuable help in form of many fruitful discussions.

References and Notes

(1) Dabrowski, J.; Kozerski, L. *Chem. Commun.* **1968**, 586; Dabrowski, J.; Kozerski, L. *J. Chem. Phys. (B)* **1971**, 345.
(2) Dabrowski, J.; Tencer, M. *Bull. Chem. Soc. Jpn.* **1975**, *48*, 1310, and references therein.
(3) Stephenson, D. S.; Binsch, G. *Quantum Chem. Prog. Exch.* **1978**, *10*, 365.
(4) Stephenson, D. S.; Binsch, G. *J. Magn. Res.* **1978**, *32*, 145.
(5) K. B. Wiberg *Acc. Chem. Res.* **1999**, *32*, 922, and references therein.
(6) Oki, M. *Applications of dynamic NMR spectroscopy to organic chemistry*; VCH Verlag: Weinheim, New York, 1985.
(7) Kessler, H. *Angew. Chem., Int. Ed. Engl.* **1970**, *9*, 219.
(8) Kleinpeter, E.; Koch, A.; Taddei, F. *THEOCHEM J. Mol. Structure* **2001**, *535*, 257.
(9) Lauvergnat, D.; Hiberty, P. C. *J. Am. Chem. Soc.* **1997**, 94788.
(10) Rablen, P. R.; Miller, D. A.; Bullock, V. R.; Hutchinson, P. H.; Gorman, J. A. *J. Am. Chem. Soc.* **1999**, *121*, 218.
(11) Bain, A. D.; Hazendonk, P.; Coutre, P. *Can. J. Chem.* **1999**, *77*, 1340.
(12) Bain, A. D.; Hazendonk, P. *J. Phys. Chem. A* **1997**, *101*, 7182.
(13) Braun, S.; Kalinowski, H.-O.; Berger, S. *100 and more basic NMR experiments*; VCH Verlag: Weinheim, New York, 1996; pp 125 and 129.
(14) Freeman, R.; Hill, H. D. W.; Kaptein, R. *J. Magn. Reson.* **1972**, 7, 327.
(15) Frisch, M. J.; Trucks, G. W.; Schlegel, H. B.; Gill, P. M. W.; Johnson, B. G.; Robb, M. A., Cheeseman, J. R.; Keith, T.; Peterson, G. A.; Oritz, J. V.; Foresman, J. B.; Cioslowski, J.; Stefanov, B. B.; Nanayakkara, A.; Challacombe, M.; Peng, C. Y.; Ayala, P. Y.; Chen, W.; Wong, M. W.; Andres, J. L.; Replogle, E. S.; Gomperts, R.; Martin, R. L.; Fox, D. J.; Binkley, J. S.; Defrees, D. J.; Baker, J.; Stewart, J. P.; Head-Gordon, M.; Gonzales, C.; Pople, J. A. *Gaussian 94*, Revision C.3; Gaussian, Inc.: Pittsburgh, PA, 1985.
(16) Tajkhorshid, E.; Paizs, B.; Suhai, S. *J. Phys. Chem. B* **1997**, *101*, 8021.
(17) Tajkhorshid, E.; Paizs, B.; Suhai, S. *J. Phys. Chem. B* **1999**, *103*, 4518.
(18) Paizs, B.; Tajkhorshid, E.; Suhai, S. *J. Phys. Chem. B* **1999**, *103*, 5388.
(19) Bernardi, F.; Garavelli, M.; Olivuci, M.; Robb, M. A. *Mol. Phys.* **1997**, *92*, 359.
(20) Tajkhorshid, E.; Suhai, S. *J. Phys. Chem. B* **1999**, *103*, 5581.
(21) Wiberg, K. B.; Rablen, P. R. *J. Am. Chem. Soc.* **1993**, *115*, 9234.
(22) Shvo, Y.; Belsky, I. *Tetrahedron* **1969**, *25*, 4649.
(23) Wiberg, K. B.; Hadad, C. M.; Rablen, P. R.; Cioslowski, J. *J. Am. Chem. Soc.* **1992**, *114*, 8644.
(24) Fischer, S.; Dunbrack, R.; Karplus, M. *J. Am. Chem. Soc.* **1994**, *116*, 11931.
(25) Prasad, B. V.; Grover, G.; Uppal, P.; Kaur, D. *THEOCHEM J. Mol. Struct.* **1999**, *458*, 227.
(26) Dabrowski, J.; Kozerski, L. *Org. Magn. Reson.* **1972**, *4*, 137.